ELSEVIER

International Journal of Refrigeration 22 (1999) 334–347

REVUE INTERNATIONALE DU FROID
INTERNATIONAL JOURNAL OF
refrigeration

Chemical dehumidification by liquid desiccants: theory and experiment

R.M. Lazzarin*, A. Gasparella, G.A. Longo

Dipartimento di Tecnica e Gestione dei Sistemi Industriale dell'Università di Padova, Viale X Giugno 22, 36100 Vicenza, Italy

Received 15 October 1997; accepted 25 April 1998

Abstract

Chemical dehumidification of air by a liquid desiccant in a packed tower has been investigated both theoretically and experimentally for air conditioning and industrial applications. A computer model of a packed tower, able to determine heat and mass transfer between air and desiccant, has been developed and a parametrical study was carried out considering the solutions H_2O/LiBr and $H_2O/CaCl_2$ to determine the optimum operative conditions. An experimental apparatus including a packed tower and a desiccant regenerator has been described together with experimental results: a set of 70 experimental runs with H_2O/LiBr. Data have been reported and compared against the results of the computer code simulations. © 1999 Elsevier Science Ltd and IIR. All rights reserved.

Keywords: Air conditioning; Lithium bromide; Calcium chloride; Absorption

Deshumidification chimique par des substances absorbantes liquides: theorie et expérimentation

Resumé

La deshumidification chimique de l'air par des substances absorbantes liquides dans une tour absorbante a eté etudié soit theoriquement soit experimentalement pour des applications dans le conditionnement de l'air et industriales. Un modèle a l'ordinateur de la tour, capable de déterminer le transfert de chaleur et de masse entre l'air et le deshumidifiant a eté développé et une étude paramétrique a considéré les solutions H_2O/LiBr et $H_2O/CaCl_2$ pour déterminer les meilleurs conditions opératives. Un circuit expérimental composé d'une tour absorbante et d'un régenerateur des absorbants est décrit et les resultats experimentaux y sont reportés. Les resultats sont comparés avec les prévisions du modèle. © 1999 Elsevier Science Ltd and IIR. All rights reserved.

Mots clés: Conditionnement d'air; Bromure de lithium; Chlorure de calcium; Absorption

Nomenclature

a	Specific interfacial surface [$m^2\ m^{-3}$]
c	Specific heat [J $(kg\ K)^{-1}$]
D	Molecular diffusivity [$m^2\ s^{-1}$]
d_s	Equivalent diameter of packing elements [m]
F	Mass transfer coefficient [kmol $(m^2\ s)^{-1}$]
G	Air mass flow rate [$kg\ s^{-1}$]
G'	Air specific mass flow rate [kg $(m^2\ s)^{-1}$]
h	Specific enthalpy [$J\ kg^{-1}$]
k	Mass transfer coefficient [kmol (m^2 s mole fraction)$^{-1}$]
L	Solution mass flow rate [$kg\ s^{-1}$]

* Corresponding author. Tel.: +39-444-9987337; fax: +39-444-998888.

PII: S0140-7007(98)00044-9

L' Solution specific mass flow rate [kg $(m^2\ s)^{-1}$]
M Molecular weight [kmol kg^{-1}]
N Specific interfacial molar flow rate [kmol $(m^2\ s)^{-1}$]
P Pressure [Pa]
q Heat flux [W m^{-2}]
r Latent heat [J kg^{-1}]
Sc Schmidt number
t Temperature [K]
X Solution concentration, [kg salt (kg solution)$^{-1}$]
X_M Molar concentration of water in the solution [kmol water (kmol solution)$^{-1}$]
Y Humidity ratio [kg water (kg dry air)$^{-1}$]
Y_M Molar concentration of water in air [kmol water (kmol air)$^{-1}$]
Z Coordinate along the column [m]
α Heat transfer coefficient [W $(m^2\ K)^{-1}$]
α' Corrected heat transfer coefficient [W $(m^2\ K)^{-1}$]
ε Void space in the packing [m^3 voids (m^3 packed volume)$^{-1}$]
ε_{L0} Operating void space in the packing [m^3 voids (m^3 packed volume)$^{-1}$]
ε_T Tower efficiency
Φ_{Lt} Total liquid holdup [m^3 liquid (m^3 packed volume)$^{-1}$]
Φ_{LO} Moving liquid holdup [m^3 liquid (m^3 packed volume)$^{-1}$]
Φ_{LS} Static liquid holdup [m^3 liquid (m^3 packed volume)$^{-1}$]
λ Thermal conductivity [W $m^{-1}\ K^{-1}$)]
μ Dynamic viscosity, [kg $(m\ s)^{-1}$]
ρ Density [kg m^{-3}]
Δ Difference

Subscripts
G Air side
i Interfacial
L Solution side
t Total
V Water vapour
0 Reference condition

1. Introduction

It is often necessary to control and modify the water vapour content in the air: the operation is quite usual in air conditioning and also in many industrial processes such as drying and preservation of some goods. Normally the water vapour content of atmospheric air is small, some tens of grams per kilo of air; nonetheless, due to the very high heat of vaporization, the latent heat content in air conditioning is of the same order of the sensible one. The relative importance of latent load increases with the ventilation rates to buildings. Higher ventilation rates are dictated both by better comfort requirements and by the most recent Standards such as the ASHRAE 62/89 [1].

Whereas the process of increasing the humidity ratio of air is relatively easily carried out with an energy cost approximately equivalent to the heat of vaporization of the added water, a humidity ratio reduction requires more complex processes. Basically two methods are at hand. The more common is the air cooling below dew point: the humidity ratio tends to reach a value close to the apparatus-dew point temperature. Cooling is usually obtained with refrigeration machinery and often some postheating is required to heat the air before it is supplied to the rooms. The other possibility is chemical dehumidification. Solid or liquid desiccants are able to reduce the water vapour content of moist air. The energy cost of the process is due to desiccant reactivation, obtained by heating, which requires low grade heat, obtainable either by a waste heat source, such as the heat recovery from an internal combustion engine, or by solar collectors. Of course regeneration can be achieved also by heat produced by a conventional burner. In dehumidification by cooling the enthalpy of eliminated vapour is normally lost to the system (unless a heat pump is operated). In chemical dehumidification this energy is available partly in the air and partly in the desiccant as sensible heat. According to the process, this heat may be useful. For example if the reactivation is carried out at pressures higher than atmospheric, heat recovery from the condensing vapour is possible at temperatures greater than 100°C. In principle, even second effect regeneration might be obtained by using a second regenerator at a lower pressure, energized by condensing vapour. Chemical dehumidification had until now few applications. The most widespread systems are desiccant wheels, which use mainly solid sorption, and packed towers which use liquid desiccants. Analyses of air conditioning and industrial drying processes showed the potential application of liquid sorbent dehumidification with possible latent heat recovery. Whereas a literature search reveals many theoretical models concerned with the performance of liquid desiccants heat/mass exchangers [2–4], experimental data are seldom reported. The few experimental studies that are reported are concerned with LiCl and $CaCl_2$ [5–7] rather than LiBr [8]. Moreover, data points are sometimes not completely specified [9].

This paper is concerned with the operation of packed bed systems. These are analysed both theoretically and experimentally, developing a computer model and surveying the operations on a testing rig realized on purpose to check the feasibility of liquid desiccant systems in air conditioning [10].

2. A computer model

A packed tower is a vertical column filled with packing such as Raschig rings or other elements with a large interfacial surface between air and liquid. The air was assumed to

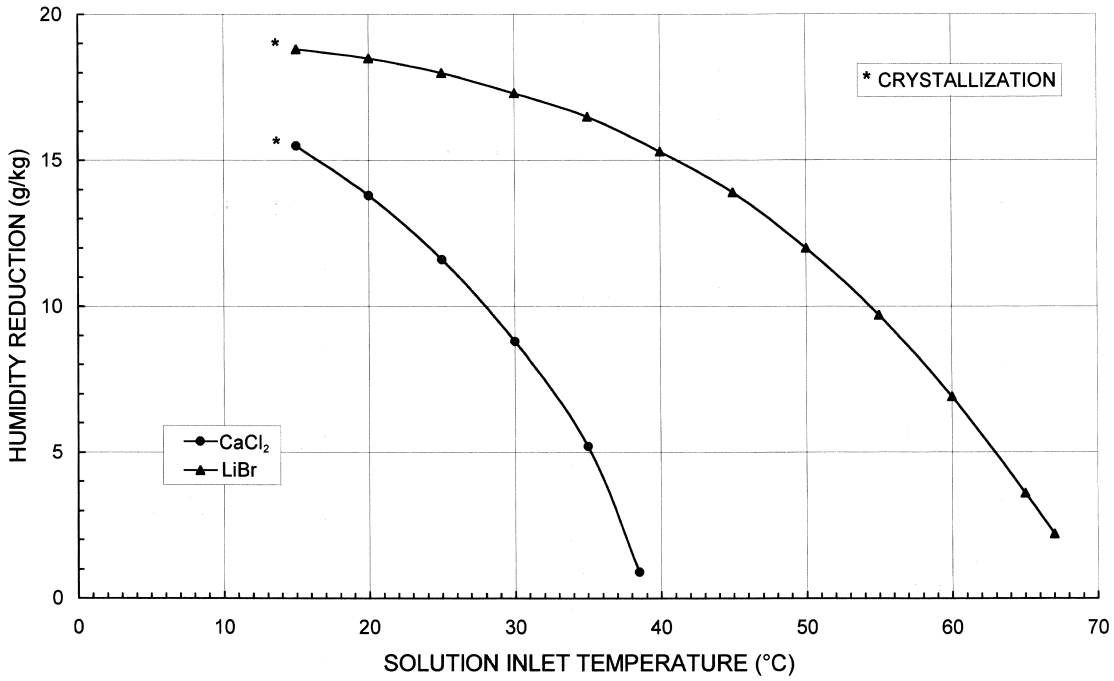

Fig. 1. Humidity reduction as a function of the inlet solution temperature.
Fig. 1. Diminution de l'humidité en fonction de la température de la solution à l'entrée.

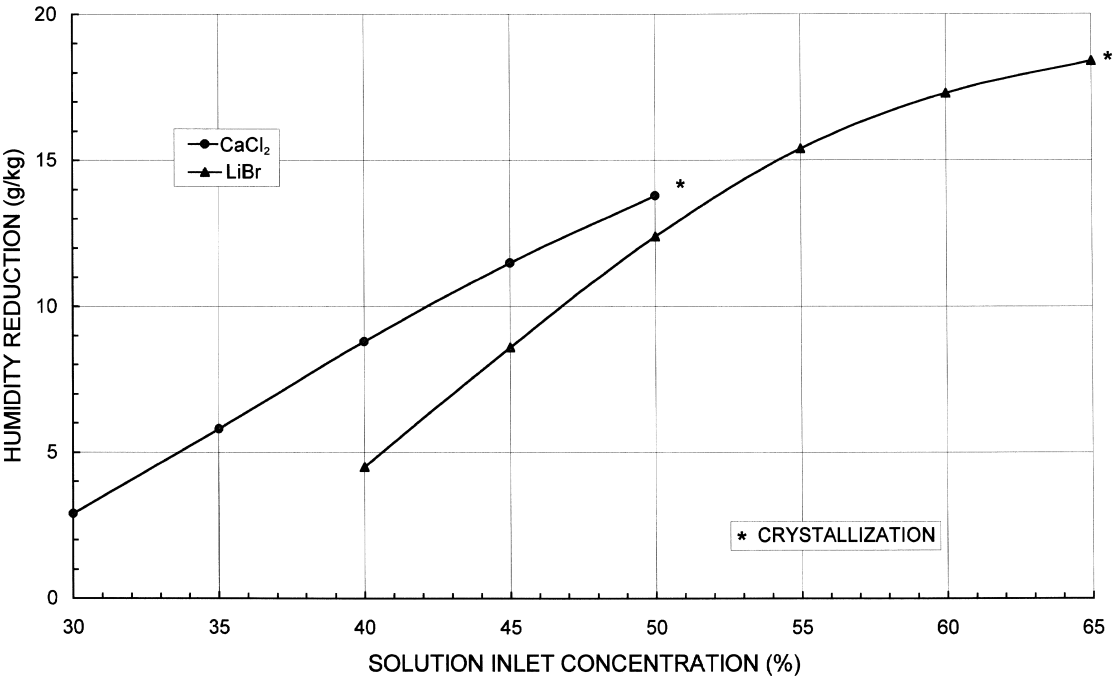

Fig. 2. Humidity reduction as a function of the inlet solution concentration.
Fig. 2. Diminution de l'humidité en fonction de la concentration de la solution à l'entrée.

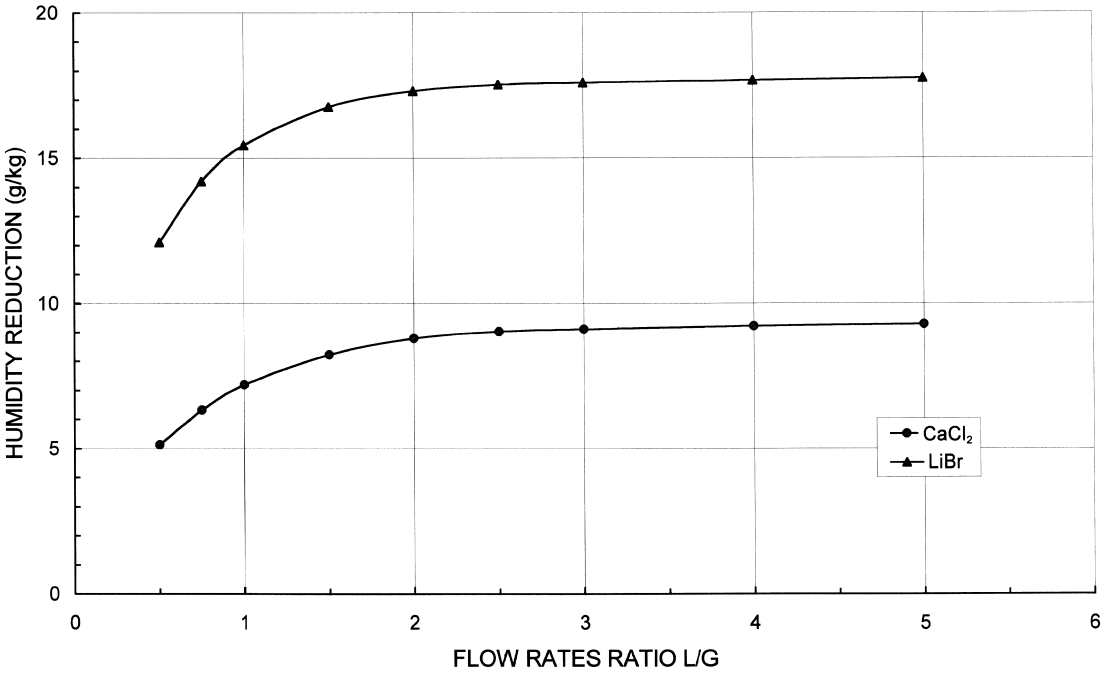

Fig. 3. Humidity reduction as a function of the flow rates ratio *L*/*G*.
Fig. 3. Diminution de l'humidité en fonction du rapport des flux L/G.

flow counter-current to the solution. The liquid, distributed over the packing, trickles down over the surface of the packing so that a large surface for contact is available to the air.

A theoretical one-dimensional analysis of an adiabatic tower with negligible liquid thermal resistance was developed. The analytical details for determining heat and mass transfer for every transversal section of the packed column are reported elsewhere [8,11,12]. Therefore, the mathematical model will be reported only briefly in Appendix A. Suitable subroutines were realized for thermophysical property calculations and the heat/mass transfer coefficient evaluation (at first of liquid desiccants $CaCl_2$–H_2O and LiBr–H_2O). The whole column is analysed by its subdivision into an appropriate number of sections. Initial assumptions on outlet conditions can be verified and adjusted by iteration. The model specifies the main characteristics of the packing. Temperature, humidity ratio and specific flow rate are supplied for the inlet air. Temperature, concentration and specific flow rate at the inlet are given with reference to the sorbent. The model computes the correspondent values at the outlet and also provides an insight into the process down the column. A parametric study was carried out to consider the experimental set-up, which will be described later. Air inlet temperature was set at 30°C with a humidity ratio of 0.020 kg $kg_{d.a.}^{-1}$ (relative humidity 75%).

Air flow rate was set at 0.1 kg s^{-1}, i.e. a specific flow rate (flow rate per unit transversal area of the tower here considered) 0.8 kg m^{-2} s^{-1}. First the influence of the inlet solution temperature was studied. Fig. 1 gives the reduction of the air humidity ratio through the column as a function of the inlet solution temperature with a solution flow rate of 0.2 kg s^{-1} (a ratio of liquid/gas mass flow rate, $L/G = 2$). The $CaCl_2$ mass concentration is 40% and the LiBr is 60% (kg salt kg solution^{-1}). These inlet concentration values were chosen since the solutions have then similar crystallization temperatures (about 11–12°C), which is far enough from the operative range. The influence of temperature is apparent. Greater dehumidification can be obtained by increasing the concentration of the solution. This is illustrated in Fig. 2, where the reduction of the air humidity ratio is given as a function of the concentration (inlet solution temperature 30°C and an $L/G = 2$). Of course the solution concentration cannot go beyond the crystallization limit.

The influence of the liquid/gas (*L*/*G*) flow rate ratio is given by Fig. 3, where the humidity ratio reduction is represented as a function of *L*/*G* ($CaCl_2$ concentration 40%, LiBr 60%, temperature 30°C). Raising this ratio higher than 2 affords little advantage, whereas lower than unity leads to a worse performance. A ratio between 1.0 and 2.5 should be maintained.

It is interesting to consider the temperature variation for the air and the solution along the tower. This temperature trend is pictured in Figs. 4a and b for the two sorbents: starting with air and solution at the same inlet temperature, the air is first heated, associated with a rapid dehumidification. This is followed by cooling, due to heat exchange with the solution.

Because the solution has a higher flow rate and specific

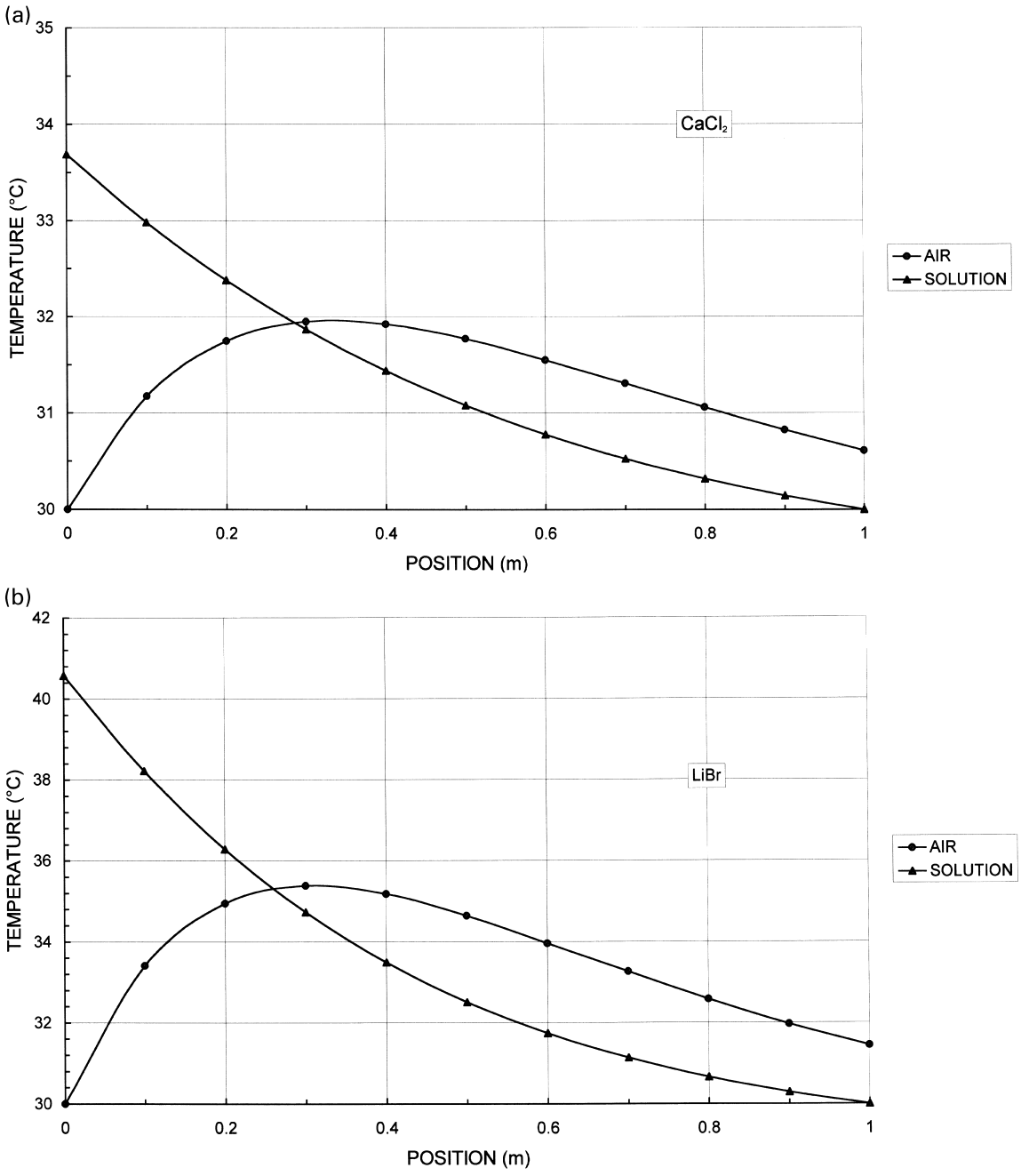

Fig. 4. (a) Solution and air temperature profiles along the tower: $CaCl_2$. (b) Solution and air temperature profiles along the tower: LiBr.
Fig. 4. (a) Profils des températures de la solution et de l'air le long de la colonne: $CaCl_2$. (b) Profils des températures de la solution et de l'air le long de la colonne: LiBr.

heat, the air temperature tends to follow that of the solution. For this reason the air temperature outlet is only slightly higher than the inlet solution. The latent heat developed in dehumidification is found as sensible heat in the solution whose outlet temperature is almost 4°C higher for $CaCl_2$ and more than 10°C for LiBr.

Dehumidification is particularly effective within the first sections of the packing after the air inlet, when the air has the highest humidity ratio, even if the solution temperature is also the highest. Consider in Fig. 5, the reduction in humidity ratio as a function of the position from the air inlet in the packing.

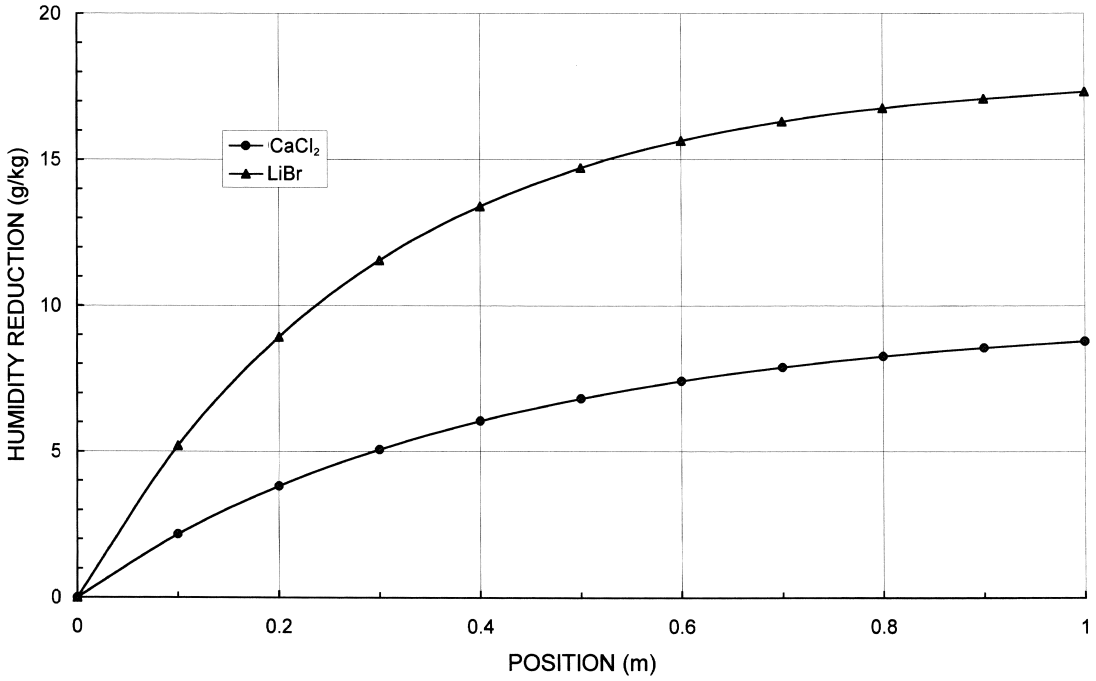

Fig. 5. Humidity reduction as a function of the position from the air inlet.
Fig. 5. Diminution de l'humidité en fonction de la position par rapport à l'entrée d'air.

Fig. 6. Real view of the experimental rig.
Fig. 6. Photo du banc d'essai.

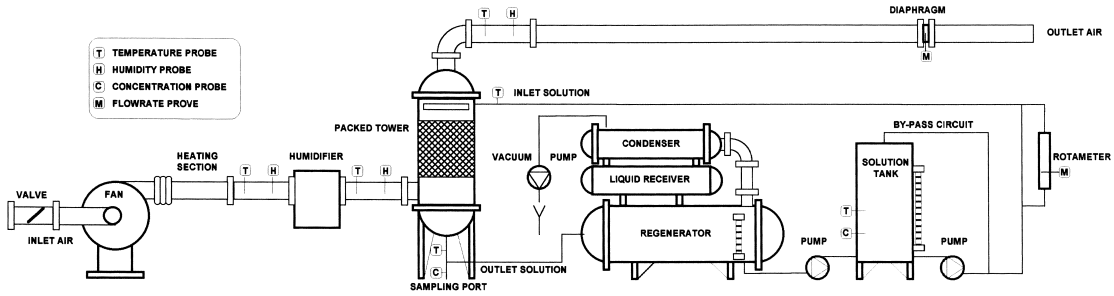

Fig. 7. Schematic diagram of the experimental rig.
Fig. 7. Schéma du banc d'essai.

The computer model was useful in fixing the experimental range. For example, the solution concentration must be greater than 45% for LiBr. However, its temperature should be lower than 40°C and, if possible, between 20 and 30°C. The specific flow rate was set from 1 to 2 kg m^{-2} s^{-1}. This choice allows a rational utilization of the column with reasonable pressure decreases. As regards the air temperature, this can be high, provided suitable values of solution concentration and temperature are selected and the humidity ratio is sufficiently great. The liquid/gas ratio should be set between 1 and 2: a slight increase in comparison with the values previously suggested allows a smaller tower height. The air specific flow rate is set between 1–2 kg m^{-2} s^{-1}.

3. Experimental apparatus and first results

The experimental apparatus (Figs. 6 and 7), consists of an air loop and a desiccant loop. The desiccant is an aqueous solution of LiBr: $CaCl_2$ is very cheap, but the ability of LiBr to dehumidify is far better. In the first loop ambient air, supplied by a fan, is heated and humidified to achieve the set conditions at the inlet of the packed tower. A fan, driven by a two-speed motor, provides an air flow rate from 0 to 400 (m^3 h^{-1}), according to the position of a damper at the fan inlet, whereas the power of the heating element can be varied from 0 to 2000 W. The steam humidifier ensures a maximum vapour flow rate of 5 kg h^{-1} with a solid state humidity control. The air goes through the packed bed, where the counterflow heat and mass transfer with the desiccant takes place and then, dehumidified and heated, it is discharged. The tower shell, made of stainless steel, 725 mm in height and 400 mm in diameter is filled with randomly packed 25 mm plastic Pall Rings supported by a stainless steel net and sprinkled by a liquid distributor. A large chamber at the bottom of the tower provides a good air distribution entering the column, whereas a stainless steel wire mesh at the top removes desiccant droplets carried out by the air at the highest velocities. An air duct, manufactured from a 160-mm diameter PVC tube, contains three measurement stations. The first of these is between the heating section and the humidifier. The remaining two are located at the inlet and the outlet of the tower to measure temperature and relative humidity. Each measuring station consists of two temperature taps instrumented with T-type thermocouples placed at different positions in the gas flow and a humidity tap containing an electronic humidity probe. The pressure drop of the air flow across the tower is measured by a U-tube manometer, while the air flow rate is measured by a diaphragm inserted in the air duct at the outlet of the tower after 3000 mm of straight tube.

The H_2O/LiBr solution is mantained at constant temperature and uniform concentration in a 200-l stainless steel tank, from where it is pumped into the tower and sprinkled onto the packed bed. The concentration of the solution is derived from density measurements by a digital densimeter.

Table 1
Specification of the different measuring devices
Tableau 1. Caractéristiques des appareils de mesure

Devices	Type	Accuracy	Operative range	Fluid
Thermometers	Thermocouples T	0.1°C	0–60°C	Air and solution
Hygrometers	Capacitive sensor	2% RH	0–95% RH	Air
Solution flowmeter	Rotameter	2%	0–500 l h^{-1}	Solution
Densimeter	Oscillator cell	1 kg m^{-3}	500–1999 kg m^{-3}	Solution
	Thermistor	0.1°C	0–40°C	
Manometer	U-tube with water	1 mm H_2O	0–200 mm H_2O	Air
Air flowmeter	Diaphragm	2%	0–800 m^3 h^{-1}	Air

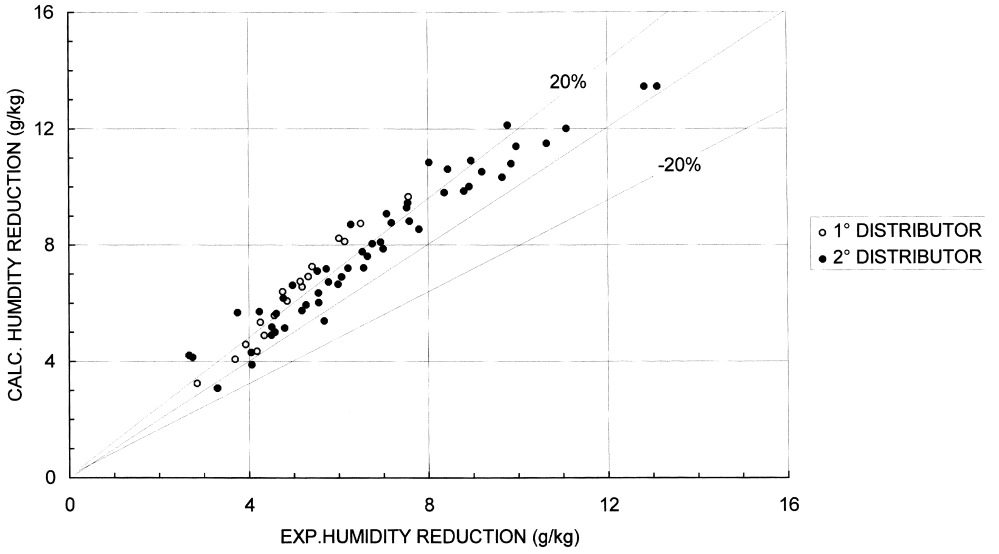

Fig. 8. Comparison between experimental humidity reduction and calculated values by the simulation program.
Fig. 8. Comparaison entre les diminutions expérimentales et prédites par le programme de simulation.

The flow rate of the desiccant, varied by the bypass valve of the tank, is measured by a rotameter and also by evaluating the variation of the liquid level in the tank in a fixed time. The solution, after the heat and mass transfer with air, collects in the bottom of the tower and flows under gravity in the regenerator. In this device the desiccant solution is regenerated by a 6000-W electric heating element controlled by solid state power module using a condenser and a vacuum pump to extract the excess water. From here the solution returns to the storage tank. The temperature of the solution is measured at the inlet and outlet of the tower by T-type thermocouples, whereas the concentration is taken at the outlet of the tower. The readings of the thermocouples and of the hygrometers are scanned and recorded by a data logger, whereas the measurements of air and desiccant flow rates and solution concentration are taken manually and then implemented into the computer. Table 1 gives the main characteristics of different measuring devices used during the experimental sessions. Only the dehumidification process is considered in this paper. The regeneration process

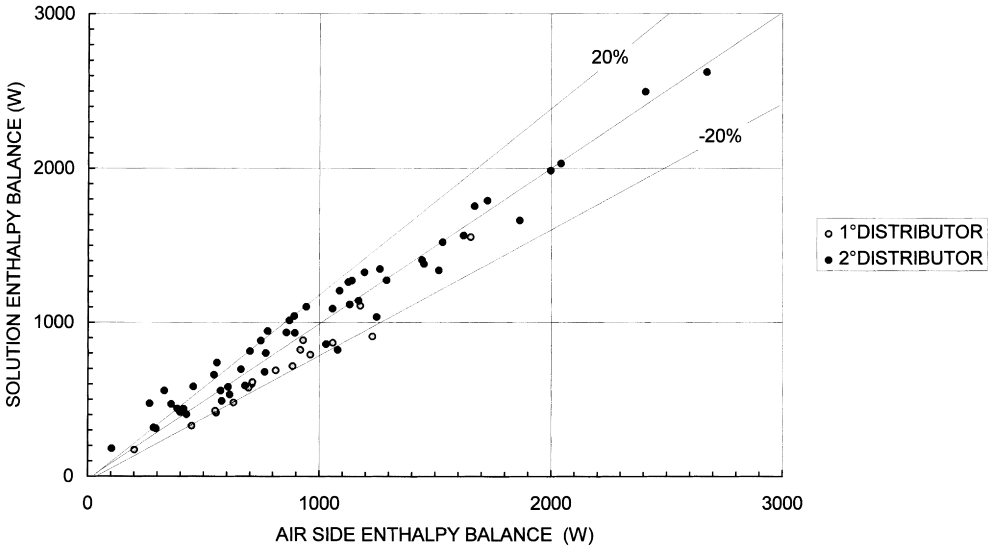

Fig. 9. Thermal balance during experimental runs: solution enthalpy balance vs air enthalpy balance.
Fig. 9. Bilan thermique pendant des essais expérimentaux: bilan enthalpiques de la solution comparé à celui du bilan enthalpique de l'air.

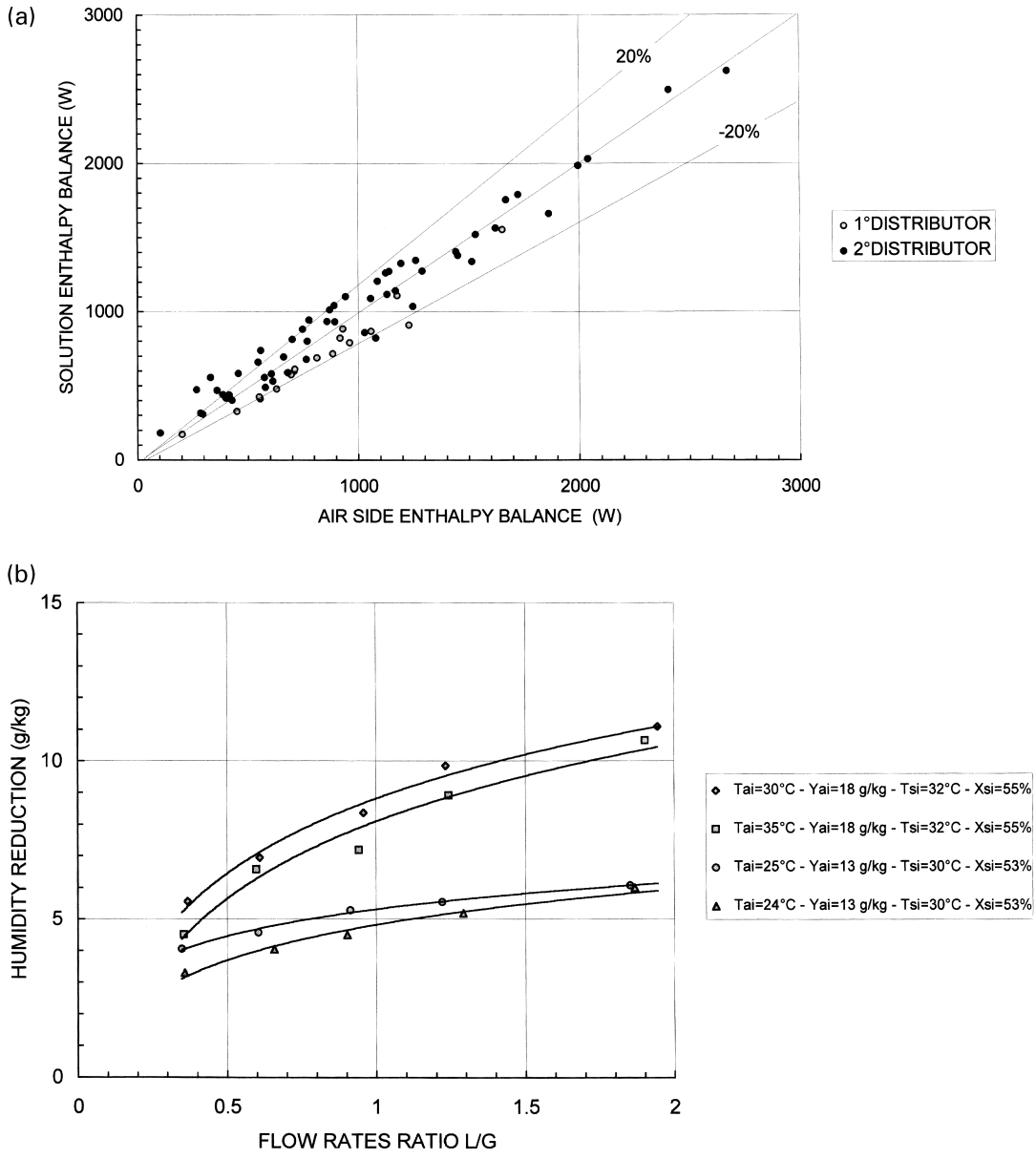

Fig. 10. (a) Humidity reduction vs flow rate ratio L/G: experimental results (second set of data and $T_{si} = 24°C$). (b) Humidity reduction vs flow rate ratio L/G: experimental results (second set of data and $T_{si} = 32°C$).

Fig. 10. (a) Diminution de l'humidité en fonction du rapport des flux L/G: résultats expérimentaux (deuxième jeu de données et $T_{si} = 24°C$). (b) Diminution de l'humidité en fonction du rapport des flux L/G: résultats expérimentaux (deuxiéme jeu de données et $T_{si} = 32°$).

is not described here. Before starting each dehumidification run the solution in the tank was recirculated through the bypass circuit to ensure uniform conditions. Then the concentration was accurately measured. The air and desiccant flow rates were then established at set values while temperature and humidity readings at different points around the rig were recorded.

Once steady state conditions of temperature and humidity were achieved, readings were collected. Whereas flow and pressure drop measurements were repeated three times, a sample of solution was taken at the outlet of the tower to measure its concentration. All these measures were implemented into the computer which calculated the heat and mass balances over the tower to determine the moisture extraction and the temperature variation for both air and solution.

The first set of 16 dehumidification runs was carried out using a liquid distributor having four spray holes, whereas the remaining set of 54 experimental data were performed

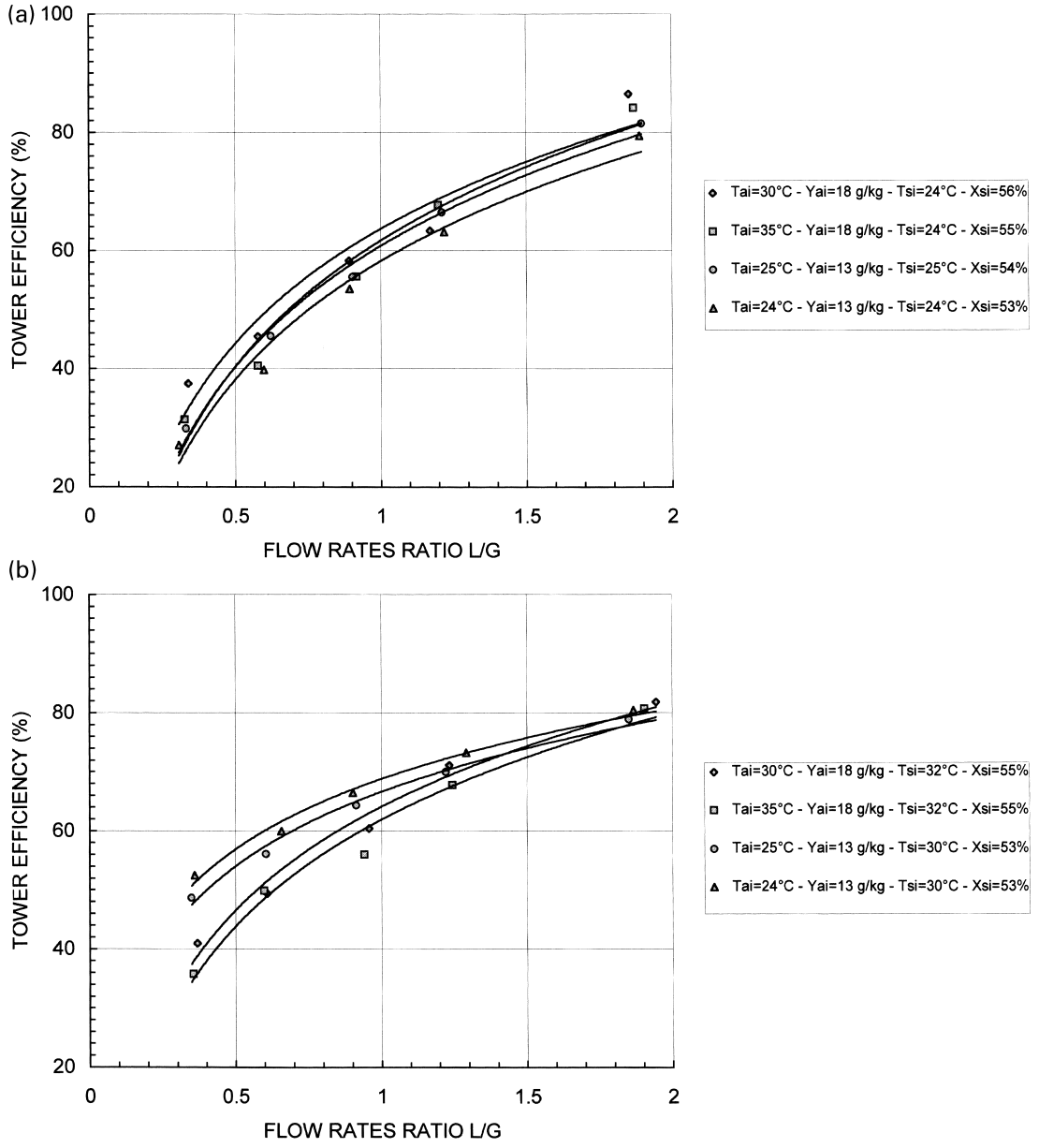

Fig. 11. (a) Tower efficiency vs flow rate ratio L/G: eperimental results (second set of data and $T_{si} = 24°C$). (b) Tower efficiency vs flow rate ratio L/G: experimental results (second set of data and $T_{si} = 32°C$).

Fig. 11. (a) Efficacité de la colonne en fonction du rapport des flux L/G: résultats expérimentaux (deuxième jeu de données et $T_{si} = 24°C$). (b) Efficacité de la colonne en fonction du rapport des flux L/G: (deuxiéme jeu de données et $T_{si} = 32°C$).

with an implemented liquid distributor having 12 spray holes. These data included air flow rate (G) at 220 $m^3\ h^{-1}$ (61.1 l s^{-1}), desiccant flow rate (L) ranging from 66 to 467 kg h^{-1} (0.0183–0.1297 kg s^{-1}), inlet air temperature (T_{ai}) from 23.6 to 35.4°C and humidity ratio (Y_i) from 10.4 to 18.7 g kg^{-1}, inlet desiccant temperature (T_{si}) from 16.1 to 34.1°C and inlet concentration (X_i) from 53 to 57% LiBr.

A detailed error analysis indicated an overall accuracy of the measured humidity reduction across the tower within 20%.

Fig. 8 shows a comparison between the experimental humidity reduction across the tower and the calculated values by the simulation program under the same operating conditions: the model overpredicts experimental data with an absolute mean deviation around 20% but with better results for the second set of data.

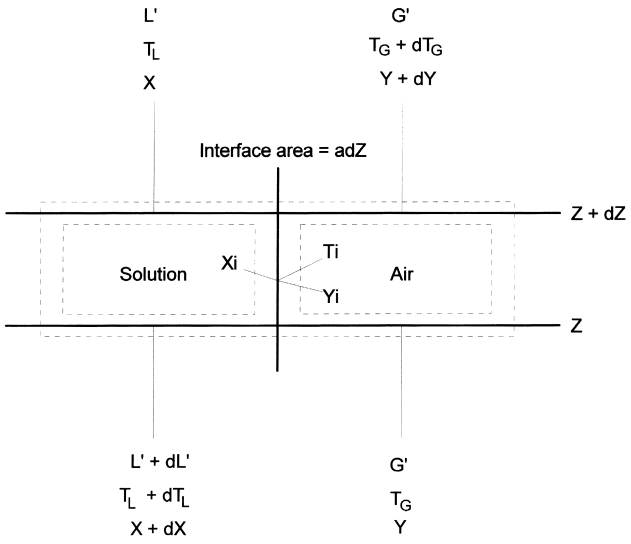

Fig. 12. Differential section of a packed column.
Fig. 12. Section différentielle d'une colonne garnie.

The assumed adiabatic conditions during experimental runs are confirmed by Fig. 9, which plots the enthalpy balance on the solution side vs the enthalpy balance on the air side across the tower: as can be seen from Fig. 9 the discrepancy is within the experimental uncertainty (less than 20%).

Figs. 10a and b illustrate the humidity reduction across the tower obtained during the second set of experimental runs as a function of the flow rate ratio (L/G) for desiccant inlet temperatures of 24 and 32°C, respectively. As can be seen the experimental trend is similar to those predicted by the computational program (Fig. 3).

Figs. 11a and b show the tower efficiency as a function of the the flow rate ratio (L/G) for the same experimental runs considered in Figs. 10a and b. The tower efficiency is equal to the ratio between the actual humidity reduction across the tower and the maximum humidity reduction possible under given conditions:

$$\varepsilon_T = (Y_{in} - Y_{out})/(Y_{in} - Y_{out.min})$$

The maximum humidity reduction is achieved when the partial vapour pressure of the air at the outlet of the tower is equal to the saturation pressure of the solution at the inlet of the tower, that is the water vapour pressure in air which has come into equilibrium with solution.

$$Y_{out.min} \Leftrightarrow P_{vap.air.out} = P_{sol.in}$$

The tower efficiency increases with the flow rate ratio up to 80–90% for the highest ratios tested, around 2. The sensitivity to this parameter is higher for the runs at the highest inlet humidity ratio.

4. Conclusions

A set of experimental surveys has been carried out on a testing rig over a wide range of air temperatures and humidities, solution temperatures, concentrations and flow rate ratios (L/G). Humidity reduction by liquid desiccants has been demonstrated, which may be useful in air conditioning [13–15].

The recorded experimental data are close to values predicted by a simple computer model. Careful design of the packed tower can improve its performance appreciably, as shown by the better results obtained by a more uniform solution sprinkling with a new distributor. In addition, other packing media are expected to perform more efficiently [16].

All the same, good tower efficiency can be obtained by choosing appropriate flow ratios in the design of a pilot air conditioning plant, while the experimental rig is useful for further analysis with other desiccants, packings and above all for the experimental of the reactivation process.

Appendix A. Mathematical model of the packed column

The theoretical model of the packed tower is based on the following assumptions:

1. the system is adiabatic,
2. the thermal resistance in the liquid phase is negligible compared with the gas phase,
3. the heat and mass transfers occur only in a transverse direction to gas and liquid flows,
4. the interface areas active in heat and mass transfer processes are the same.

The enthalpy of the desiccant with respect to a reference temperature t_0 results:

$$h_L = c_L(t - t_0) + h_S \quad (1)$$

where c_L is the specific heat and h_S the dilution heat of solution at the reference temperature. For humid air the specific enthalpy is:

$$h_G = c_G(t - t_0) + Y[c_V(t_G - t_0) + r_0] \quad (2)$$

with Y the humidity ratio, c_G and c_V specific heat for dry air and steam, respectively, and r_0 water latent heat at the reference temperature.

Fig. 12 shows a differential control volume of the tower 1 m^2 in cross section area and dZ in height: the heat and mass transfer takes place at the interface between solution and air in a counterflow configuration. The mass conservation equation for the water content gives:

$$dL' = G'dY \quad (3)$$

where L' and G' are the specific mass flow rate (kg $(m^{-2}\ s)^{-1}$) for the liquid and gas phases. The mass transfer at the interface gives:

$$N_V M_V a dZ = -G'dY \quad (4)$$

where 'a' is the specific interfacial surface (m^2 of interface per m^3 of packed volume) function of packing structure, M_V is the molecular weight of water and N_V the specific interfacial molar flow rate (kmol $(m^{-2}\ s)^{-1}$). This parameter can be related to the interfacial Y_{Mi} and bulk Y_M molar concentration of water in air flow by the following correlation:

$$N_V = F_G \ln[(1 - Y_{Mi})/(1 - Y_M)] \quad (5)$$

where F_G is the mass transfer coefficient relative to the gas phase (kmol $(m^{-2}s)^{-1}$). The molar concentration Y_M is correlated to the humidity ratio by the relation:

$$Y_M = p_{vG}/p_t = Y/(Y + M_V/M_G) \quad (6)$$

with p_{vG} and p_t vapour partial pressure and total pressure in humid air, and M_G the molecular weight of dry air. If the interfacial mass transfer resistance in the liquid phase is negligible, the interfacial vapour pressure is equal to that in the solution and Eq. (5) becomes:

$$N_V = F_G \ln[(1 - p_{vL}/p_t)/(1 - p_{vG}/p_t)] \quad (7)$$

The mass transfer coefficient F_G can be computed by the following empirical correlation [11]:

$$F_G = 1.195G\{d_s G'/[\mu_G(1 - \varepsilon_{L0})]\}^{-0.36} Sc^{-0.667} \quad (8)$$

where d_S is the equivalent diameter of the packing elements reported in Table 2, μ_G is the gas dynamic viscosity and ε_{L0} is the operating void space in the packing equal to void space of the dry packing minus the total liquid holdup:

$$\varepsilon_{L0} = \varepsilon - \Phi_{Lt} \quad (9)$$

$$\Phi_{Lt} = \Phi_{LO} + \Phi_{LS} \quad (10)$$

The total liquid holdup consists of the 'moving holdup' Φ_{LO} (liquid retained in the packing and continually replaced by fresh liquid) and the 'static holdup' Φ_{LS} (liquid retained in the interstices of the packing and only slowly replaced by fresh liquid): Table 2 gives some holdup correlations for different packing elements.

The Schmidt number is the equivalent for mass transfer to the Prandtl number for heat transfer and results:

$$Sc_G = \mu_G/\rho_G D_G \quad (11)$$

with ρ_G and D_G the density and molecular diffusivity of air, respectively.

The interfacial area for absorption with water or aqueous solutions can be evaluated by the following equation [11]:

$$a_A = m(808\ G'/\rho_G^{0.5})^n L'^p \quad (12)$$

The coefficients m, n and p are given in Table 2, L' is the liquid specific flow rate.

From Eq. (4) and Eq. (5) we obtain:

$$-G'dY = (M_V F_G a dZ)\ln[(1 - Y_{Mi})/(1 - Y_M)] \quad (13)$$

and so the basic differential equation for the mass transfer gives:

$$(dY/dZ) = -(M_V F_G a/G')\ln[(1 - Y_{Mi})/(1 - Y_M)] \quad (14)$$

The interfacial molar concentration Y_{Mi} in the gas phase can be calculated by considering the mass balance at the interface. The specific interfacial mass transfer on the solution side gives:

$$N_L = F_L \ln[(1 - X_M)/(1 - X_{Mi})] \quad (15)$$

where X_M and X_{Mi} are the bulk and interfacial molar concentration in water of the solution, while F_L is the mass transfer coefficient in the liquid phase equal to:

$$F_L = k_L(\rho_L/M_L)X_{MBM} \quad (16)$$

X_{MBM} is the average molar concentration in salt of the solution, while M_L is the average molecular weight of the solution. The liquid-phase mass transfer coefficient k_L can be calculated by the following empirical correlation [11]:

$$k_L = 25.1(D_L/d_s)(d_s L'/\mu_L)^{0.45} Sc_L^{0.5} \quad (17)$$

where the Schmidt number for the solution is:

$$Sc_L = \mu_L/\rho_L D_L \quad (18)$$

with D_L molecular diffusivity of liquid phase.

By equating the specific interfacial mass transfer on the gas side (Eq. 5) to that on the liquid side (Eq. 15) it is possible to derive the following expression for the interfacial molar concentration in water on the air side:

$$Y_{Mi} = 1 - (1 - Y_M)[(1 - X_M)/(1 - X_{Mi})]^{F_L/F_G} \quad (19)$$

This equation has to be solved simultaneously with the vapour–liquid equilibrium equation for the solution by an iterative procedure.

Table 2
Liquid holdup and interfacial areas of absorption in the packed column [11].
Tableau 2. Rétention du liquide et surfaces d'interface d'absorption dans la colonne garnie.

Packaging element	Nominal dimension	Diameter d_s (m)	e	Flow rate L' (kg m^{-2}s^{-1})	Constant for computation of a_A			Holdup Φ
					m	n	p	
Raschig Rings: Ceramic	1′ 25 mm	0.0356	0.730	0.68–2.0	34.42	0	0.552	$\beta = 1.508\, d_s^{0.376}$
				2.0–6.1	68.20	$0.0389L' - 0.0793$	− 0.470	
	2′ 50 mm	0.0725	0.740	0.68–2.0	31.52	0	0.481	$\Phi_{LT} = \dfrac{2.09\times10^{-6}(737.5L')^{\beta}}{d_s^2}$
				2.0–6.1	34.03	0	0.362	
RaschigRings:Carbon	1′ 25 mm	0.01301	0.745	0.68–2.0	34.42	0	0.552	$\beta = 1.104\, d_s^{0.376}$
				2.0–6.1	68.20	$0.0389L' - 0.0793$	− 0.470	
	2′ 50 mm	0.0716	0.730	0.68–2.0	31.52	0	0.481	$\phi_{LT} = \dfrac{7.34\times10^{-6}(737.5L')^{\beta}}{d_s^2}$
				2.0–6.1	34.03	0	0.362	
Berl.Saddles:Ceramic	1′ 25 mm	0.0320	0.690	0.68–2.0	52.14	$0.0506L' - 0.1029$	0	$\beta = 1.508\, d_s^{0.376}$
				2.0–6.1	73.00	$0.0310L' - 0.0630$	− 0.359	
	1.5′ 38 mm	0.0472	0.750	0.68–2.0	40.60	− 0.0508	0.455	$\Phi_{LT} = \dfrac{2.32\times10^{-6}(735.5L')^{\beta}}{d_s^2}$
				2.0–6.1	62.40	$0.0240L' - 0.0996$	− 0.1355	

The simultaneous heat transfer gives:

$$q_G a dZ = \alpha'_G a(t_G - t_i)dZ \quad (20)$$

where q_G is the sensible heat flux on the gas side (W m^{-2}); α'_G is the gas heat transfer coefficient corrected to account for simultaneous mass transfer (Ackermann correction), t_G and t_i are the bulk and interfacial air temperature. The Ackermann correction for simultaneous mass transfer gives:

$$\alpha'_G a = N_V M_V c_V a/[1 - \exp(-N_V M_V c_V a/\alpha_G a)] \quad (21)$$

Considering Eq. (4) it gives:

$$\alpha'_G a = -G' c_V (dY/dZ)/[1 - \exp(G' c_V (dY/dZ)/\alpha_G a] \quad (22)$$

The heat transfer coefficient for air α_G can be calculated by the following equation:

$$\alpha_G = 1.195\, G' c_G \{d_s G'/[\mu_G (1 - \varepsilon_{L0})]\}^{-0.36} (\mu_G c_G/\lambda_G)^{-0.667} \quad (23)$$

derived by the analogy between heat and mass transfer from Eq. (8): the Schmidt number in Eq. (8) has been replaced by the Prandlt number $\mu_G c_G/\lambda_G$.

Now we can establish a thermal balance on the air side in the following form:

$$G' h_G - G'(h_G + dh_G) + G' dY[c_V(t_G - t_0) + r_0] = \alpha'_G a(t_G - t_i)dZ \quad (24)$$

where the enthalpy variation of air across the differential element gives:

$$dh_G = c_G dt_G + Y c_V dt_G + dY[c_V(t_G - t_0) + r_0] \quad (25)$$

Rearranging Eq. (24) and Eq. (25) we obtain the basic differential equation for heat transfer:

$$(dt_G/dZ) = -\alpha'_G a(t_G - t_i)/[G'(c_G + Y c_V)] \quad (26)$$

Now we have the relations (Eq. (14) and Eq. (26)) to compute the humidity and temperature gradients along the packed column on the air side and we can establish an overall thermal balance for the adiabatic system solution–air, exactly:

$$L' dh_L + G' dY\, h_L = G' dh_G \quad (27)$$

Eq. (1) and Eq. (24) give:

$$L'[c_L dt_L + d(\Delta h_S)] + G' dY[c_L(t_L - t_0) + \Delta h_S] = \{c_G dt_G + Y c_V dt_G + dY[c_V(t_G - t_0) + r_0]\} G'$$

Neglecting the variation of diluition heat $d(h_S)$ we obtain the solution temperature gradient across the column:

$$(dt_L/dZ) = (G'/L' c_L)\{(c_G + Y c_V)(dt_G/dZ) + [c_V(t_G - t_0) + r_0](dY/dZ) - [c_L(t_L - t_0) + h_S](dY/dZ)\} \quad (28)$$

So we have the differential equation for all the characteristic parameters of both the flows and we can simulate the packed column section by section.

Thermodynamical, thermophysical and transport properties of the desiccant solutions considered, H_2O/LiBr and $H_2O/CaCl_2$, have been calculated in accordance with Refs. [17–19].

References

[1] ASHRAE Standard 62/89. Ventilation for acceptable air quality.

[2] Zografos AI, Petroff C. A liquid desiccant dehumidifier performance model. ASHRAE Trans.: Symposia, 650-656, NY-91-8-3.

[3] Lowenstein AI, Dean MH. The effect of regenerator performance on a liquid desiccant air conditioner. ASHRAE Trans 1992;98:704–711.

[4] Lowenstein AI, Gabruk RS. The effect of absorber design on the performance of a liquid-desiccant air conditioner. ASHRAE Trans 1992;98:712–720.

[5] Patnaik S, Lenz TG, Löf GOG. Performances studies for an experimental solar open-cycle liquid desiccant air dehumidification system. Solar Energy 1990;44:123–135.

[6] Khan AY, Ball HD. Experimental performance verification of a coil-type liquid desiccant system at part-load operation. Solar Energy 1993;51:401–408.

[7] Ertas A, Gandhidasan P, Kiris I, Anderson EE. Experimental study on the performance of a regeneration tower for various climatic conditions. Solar Energy 1994;53:125–130.

[8] Factor HM, Grossman G. A packed bed dehumidifier/regenerator for solar air conditioning with liquid desiccants. Solar Energy 1980;24:541–550.

[9] Stevens DI, Braun JE, Klein SA. An effectiveness model of liquid-desiccant system heat/mass exchangers. Solar Energy 1989;42:449–455.

[10] Lazzarin RM, Longo GA. Chemical dehumidification by liquid desiccant: an experimental analysis. Proc 19th Int Cong of Refrg, The Hague, 1995;3b:816–823.

[11] Treybal R. Mass transfer operations, 3rd ed. New York: McGraw Hill, 1980:187–219.

[12] Gandhidasan P, Kettelborough CF, Rifat Ullah M. Calculation of heat and mass transfer coefficients in a packed tower operating with desiccants–air contact system. J Solar Energy Eng 1986;108:123–128.

[13] Lazzarin R, Longo GA. Open cycle absorption: a simple route to gas-fired cooling and heating. IEA Heat Pump Centre Newsletter 1992;10:12–15.

[14] Lazzarin RM, Longo GA, Romagnoni PC. A new HVAC system based on cogeneration by an i.c. engine. Applied Thermal Eng 1996;16:551–559.

[15] Lazzarin RM, Longo GA, Gasparella A. Theoretical analysis of an open-cycle absorption heating and cooling system. Int J Refrig 1996;19:160–167.

[16] Bomio P. Sulzer Columns for absorption and desorption processes. Sulzer Technical Review 1979;62–68.

[17] Mcnelly L. Thermodynamic properties of aqueous solutions of lithium bromide. ASHRAE Trans. 1979;85:412–434.

[18] Lower H. Thermodynamische eigenschaften und warmediagramme des binaren systems lithiumbromid wasser. Kaltetechnik May 1961:178–184.

[19] Lower H. Dichte, spezifische warme, warmeleitzahl, dynamische viskosität der wasseringen lithiumbromid lösung. Kältetechnik, September 1961, October 1961, March 1962.